

Cite this article: Roomul Mashtaq, Towseef Ahmad, Shahbaz Ahmad, Mohd Zubair Ansari, Structural, optical and morphological properties of solvothermally synthesized CZTS nanomaterials, *RP Cur. Tr. Appl. Sci.* 3 (2024) 56–59.

Original Research Article

Structural, optical and morphological properties of solvothermally synthesized CZTS nanomaterials

Roomul Mushtaq, Towseef Ahmad, Shahbaz Ahmad, Mohd Zubair Ansari*

Department of Physics, National Institute of Technology Srinagar, Hazratbal Srinagar, Jammu and Kashmir, 190006, India

*Corresponding author, E-mail: mohdzubair@nitsri.ac.in

ARTICLE HISTORY

Received: 25 June 2024
Revised: 28 August 2024
Accepted: 30 August 2024
Published online: 1
September 2024

KEYWORDS

CZTS; Kesterite; Polygonal nanoparticles; Crystallite size; Agglomeration.

ABSTRACT

Cu₂ZnSnS₄ (CZTS) nanomaterials has seen substantial usage in solar cell research due to its significant absorption coefficient approximately 10⁴ cm⁻¹, appropriate band gap 1.5 eV in the visible spectrum, great potential as a p-type semiconductor material, good photo stability, the relative quantity of the component elements and their nontoxicity. This work presents the results of our investigation into the structural, morphological, and optical properties of p-type kesterite CZTS nanocrystal powder, which was produced by solvothermal technique. The sharp XRD (X-ray diffractometer) peaks show that the material is highly crystalline, with crystallite size close to 10 nm. The optical band gap of the produced nanomaterial is 1.53 eV, which is close to the usual 1.52 eV value. The morphology of CZTS nanostructures was examined using field emission scanning electron microscopy (FESEM). The image clearly shows that the material is equally distributed with polygonal nanoparticles and agglomerated morphology.

1. Introduction

One of the most abundant and environmentally responsible ways to create electrical energy nowadays is through the utilization of regenerative sources of energy [1]. In nowadays most of the solar industry is made up of Silicon (Si) based solar cells. This is because of the versatility of Si in its properties like durability, nontoxic nature, and abundance in earth's crust. Low absorption coefficient is the only factor in Si based solar cells, which inserts room for future efficiency improvements. In the meantime, lot of research is going for high efficiency solar cell materials alternate to Si based solar cell material. New materials with high absorption coefficient like CdTe, CIGS, CZTS has been developed. The solar cells based on CdTe and CIGS has not been without challenges. The hazardous effects of Cd, Te, Se and limited availability of In, Te in the earth's crust are the big challenges that need to be completed [2]. The above-mentioned novel material CZTS (Cu₂ZnSnS₄) finds too much room to fulfill the challenges. It has high absorption coefficient 10⁴ cm⁻¹ and tunable bandgap from (1.4 - 1.8 eV) [3]. The nature of its elements is nontoxic and abundance is much in the crust of earth. Because of these properties it has variety of applications in photocatalysis, photodetection, supercapacitor, PEC hydrogen production etc.

In this study, solvothermal synthesis of CZTS has been opted. It is one pot synthesis method without the addition of any other antecedents to accomplish the growth. It is simple and cost-effective process thus; this technique is perfect for mass production of CZTS nanoparticles. Structural analysis was done to conform the phase. Optical bandgap and morphology were visualized so that material can be applicative.

2. Materials and methods

2.1 Materials

The reagents used in analysis, including copper (II) acetate monohydrate ((CH₃COO)₂Cu.H₂O), and zinc acetate pentahydrate ((CH₃COO)₂Zn.5H₂O) were procured from Rankem, stannouschloride dihydrate (SnCl₂.2H₂O) was procured from CDH and thiourea (CH₄N₂S) was purchased from Merck.

2.2 Methods

To synthesize CZTS nanoparticles solvothermal method was opted. The precursor solution of Cu, Zn, Sn, and S i.e. (CZTS) was prepared using 0.02M copper (II) acetate monohydrate ((CH₃COO)₂Cu.H₂O), 0.01M zinc acetate pentahydrate ((CH₃COO)₂Zn.5H₂O), 0.01M tinchloride dihydrate (SnCl₂.2H₂O), and 0.08M thiourea (CH₄N₂S) in 50 ml of ethylene glycol kept on magnetic stirrer with hot plate with temperature 45°C. The pH of the desired solution i.e. CZTS was adjusted to 8 with the precursor ratio 2:1:1:8. The solution was vigorously stirred for 2 hours. Afterwards, it was transferred in a stainless-steel autoclave that was lined with Teflon, it was closed tightly and kept at 170°C for 24 hours. After cooling down to room temperature, nanoparticles were washed and centrifuged several times first with di water and then with absolute ethanol. Later the product was dried off overnight at 70°C. After that the product was grounded and stored in a vial that remains unchanged even after long-term storage before further characterizations.



3. Characterizations

Rigaku with source Cu K α ($\lambda = 1.54 \text{ \AA}$) X-ray diffractometer (XRD) was used to illustrate the phase and structure of the synthesised CZTS nanoparticles. The Gemini Zeissultra 55 FESEM and EDAX have been used for high resolution image and elemental analysis. Synthesised CZTS nanoparticles' band-gap was determined with the use of a Tauc plot, and their optical properties were examined with Perkin Elmer Lambda 365 UV-Visible Spectrophotometer.

4. Results and discussion

4.1 Phase analysis of CZTS nanoparticles

The crystalline structure and phase of the synthesized CZTS nanomaterial were revealed by X-ray diffraction analysis, as shown in Figure 1. The primary peaks at diffraction angles of 28.56°, 32.93°, 47.45°, 56.31°, 69.30°, and 76.47°, which correspond to reticular planes (112), (200), (220), (312), (008), and (332), respectively, are seen in these spectra and correspond to crystalline tetragonal kesterite phase as given in JCPDS No-26-0575 [4 – 6].

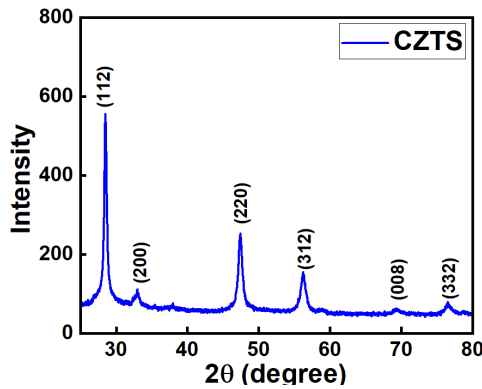


Figure 1: XRD patterns of CZTS nanoparticles synthesized by solvothermal method.

To obtain the crystallite size (D) Scherrer equation was used [3]:

$$D = k\lambda/\beta \cos(\theta) \quad (1)$$

where k is constant ($k = 0.9$), λ is the wavelength of incident X-ray radiation, β is the full width at half of the maximum (FMHW) and θ is Bragg angle. The crystallite size (D) of CZTS nanoparticles was obtained as ~ 10 nm and the corresponding lattice parameters obtained were $a = b = 0.54$ nm and $c = 1.08$ nm by using the expression:

$$1/d^2 = (h^2 + k^2) / a^2 + l^2 / b^2 \quad (2)$$

where d is inter planar spacing and can be obtained from the equation:

$$2d \sin \theta = n\lambda \quad (3)$$

where θ , λ are same as mentioned in the equation (1) and $n = 1$ (order of diffraction).

The observed values of lattice parameters a , b and c match well with the standard values obtained from JCPDS card 26-

0575. The standard and observed " d_{hkl} " values corresponding to their respective plane, 2θ values, and lattice parameters are summarized in the Table 1.

Table 1: Observed values of lattice parameters of CZTS nanomaterials.

Sr.no.	2 θ (in degree)		Plane (hkl)	"d" spacing (in nm)	
	Standard	Observed		Standard	Observed
1	28.53	28.56	(112)	0.312	0.312
2	32.99	32.93	(200)	0.271	0.271
3	47.33	47.45	(220)	0.191	0.191
4	56.17	56.31	(312)	0.163	0.163
6	69.22	69.30	(008)	0.135	0.135
7	76.43	76.47	(332)	0.124	0.124

4.2 Optical properties

A Tauc plot and optical absorbance spectra of CZTS nanoparticles are shown in Figure 2(a). As the picture shows, the material absorbs nearly the entire visible spectrum. Since CZTS nanoparticles are black in color, they absorb light over much of the visible spectrum. Linking the photon energy ($h\nu$) to the optical absorption coefficient (α) i.e. Tauc plot was obtained using the absorbance data [7].

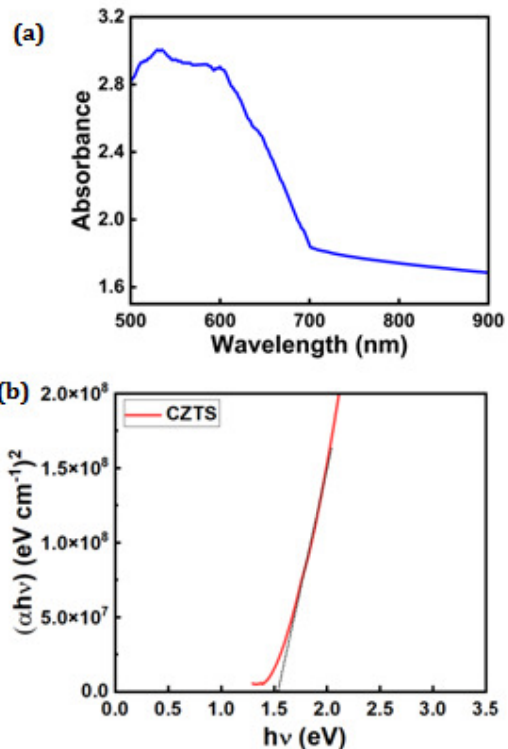


Figure 2: (a) Absorption spectrum of CZTS nanomaterial plotted against wavelength;

(b) Tauc plot for band gap calculation of CZTS nanoparticles.

The optical bandgap E_g of the CZTS nanomaterial can be given by the following relation [9]:

$$\alpha h\nu = A (h\nu - E_g)^n \quad (4)$$

here this context, A is a constant, θ is the transition frequency, and the nature of the band transition is determined by the exponent n , where $n = 1/2$ and $3/2$ correspond to direct permitted and direct forbidden transitions, respectively, and $n = 3$ and 2 correspond to indirect forbidden and indirect allowed transitions, respectively [10]. The optical band-gap E_g was noted while extending the linear segment of $(\alpha h\nu)^2$ vs. $h\nu$ curve to $\alpha = 0$ with $n = 1/2$ the calculated band gap of the sample was turned out to be 1.53 eV as depicted in Figure 2(b).

4.3 Morphology and compositional analysis

The ratio of the atoms i-e Cu, Zn, Sn, and S are 2.02:1.09:1:4.23, as determined by semi-quantitative EDS analysis well exhibited from Figure 3. The 2:1:1:4 ratio and the empirical formula of Cu_2ZnSnS_4 are well-supported by this.

Similar to a literature, the synthesized CZTS exhibits a certain level of Sulfur deficiency, which impacts its structural and morphological properties and also results in the formation of secondary phases [11]. Here, the absence of other elements in the as-synthesized CZTS nanomaterial apart from Cu, Zn, Sn, and S is the reflection for the phase purity of CZTS nanomaterials.

The morphology of CZTS nanostructures was visualized by field emission scanning electron microscopy. Figure 4 (a) and (b) shows the FESEM images the CZTS nanostructure that was synthesized. There are consistently dispersed polygonal nanoparticles throughout the sample, as seen in the micrograph with agglomerated nature. The agglomeration can be attributed due to composition ratio of the solution mixture [12].

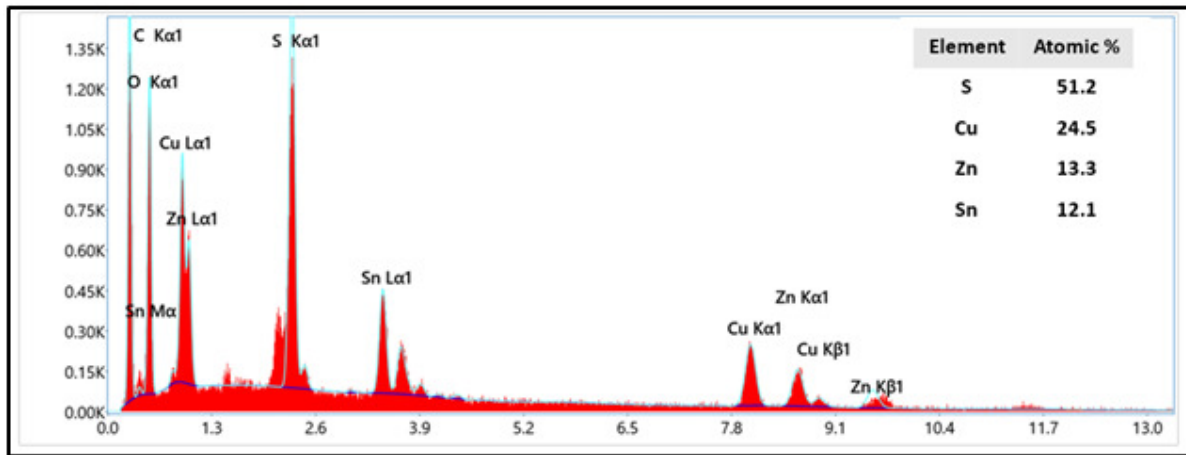


Figure 3: Energy dispersive X-ray analysis spectrum of CZTS nanoparticles, inset shows the elemental composition of Cu, Zn, Sn, and S elements in CZTS.

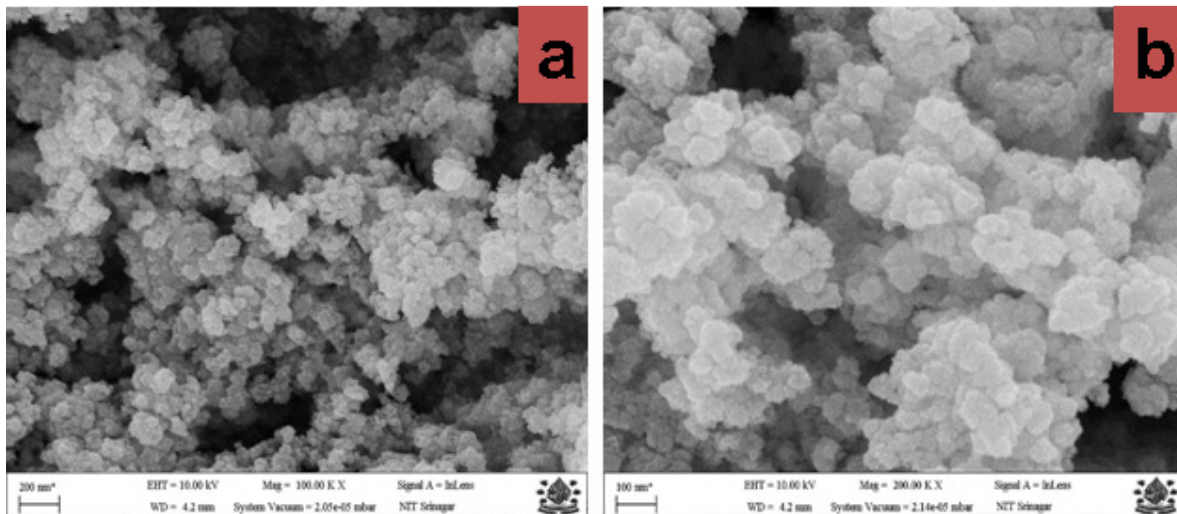


Figure 4: FESEM images of CZTS at (a) low and (b) high magnifications.

5. Conclusions

Synthesis of CZTS nanomaterials using one pot solvothermal method has been stated. The confirmation of the creation of a quaternary semiconductor within the kesterite structure with a favored (112) orientation was achieved using XRD investigation with crystallite size 10 nm. Their optical

bandgap in the visible range was found to be around 1.53 eV for the nanomaterial. Field emission scanning electron microscopy (FESEM) was used to examine the morphology of CZTS nanostructures. The results demonstrate that the sample is uniformly distributed with polygonal nanoparticles. The atomic ratio was analyzed using EDS and observed ratio was

24.5:13.3:12.1:51.2 = 2.02:1.09:1:4.23 for copper (Cu), zinc (Zn), tin (Sn) and sulfur (S) elements that are consistent with the empirical formula of $\text{Cu}_2\text{ZnSnS}_4$. Due to its exceptional purity, as-synthesized CZTS nanoparticles show no traces of any other elements in the EDS pattern.

References

- [1] Y. Majeed, M.U. Khan, M. Waseem, U. Zahid, F. Mahmood, F.F. Majeed, M. Sultan, A. Raza, Renewable energy as an alternative source for energy management in agriculture, *Energy Rep.* **10** (2023) 344-359.
- [2] X. Yu, A. Shavel, X. An, Z. Luo, A. Cabot, $\text{Cu}_2\text{ZnSnS}_4$ - Pt and $\text{Cu}_2\text{ZnSnS}_4$ - Au heterostructured nanoparticles for photocatalytic water splitting and pollutant degradation, *J. Am. Chem. Soc.* **136** (2014) 9236–9239.
- [3] M.Z. Ansari, M. Faraz, S. Munjal, V. Kumar, N. Khare, Highly dispersible and uniform size $\text{Cu}_2\text{ZnSnS}_4$ nanoparticles for photocatalytic application, *Adv. Powder Technol.* **28** (2017) 2402-2409.
- [4] M.Z. Ansari, N. Khare, Rapid synthesis of flower shaped $\text{Cu}_2\text{ZnSnS}_4$ nanoparticles by microwave irradiation for solar cell application, *AIP Conf. Proc.* **1728** (2016) 1-5.
- [5] J. Wang, P. Zhang, X. Song, L. Gao, Surfactant-free hydrothermal synthesis of $\text{Cu}_2\text{ZnSnS}_4$ (CZTS) nanocrystals with photocatalytic properties, *RSC Adv.* **4** (2014) 27805-27810.
- [6] S. Kumar, M.Z. Ansari, N. Khare, Enhanced thermoelectric power factor of $\text{Cu}_2\text{ZnSnS}_4$ in the presence of Cu_{2-x}S and SnS_2 secondary phase, *AIP Conf. Proc.* **1832** (2017) 1-4.
- [7] D.K. Maurya, S. Sikarwar, P. Chaudhary, S. Angaiyah, B.C. Yadav, Synthesis and characterization of nanostructured copper zinc tin sulphide (CZTS) for humidity sensing applications, *IEEE Sens. J.* **19** (2019) 2837-2846.
- [8] M.G.C. Beh, B. Hartiti, A. Ziti, F.K. Konan, A. Batan, H. Labrim, A. Laazizi, C.T. Haba, P. Thevenin, Optical and structural properties of CZTS thin films produced by electrodeposition, *Mater Today Proc.* 2024 (In Press). doi:10.1016/j.matpr.2024.03.029.
- [9] T. Ahmad, M.Z. Ansari, Structural and optical characteristics of Sb doped SnO_2 nanoparticles and their boosted photocatalytic activity under visible light irradiation, *Ceram. Int.* **49** (2023) 35740-35756.
- [10] S. Sikarwar, B.C. Yadav, S. Singh, G.I. Dzhardimalieva, S.I. Pomogailo, N.D. Golubeva, A.D. Pomogailo, Fabrication of nanostructured yttria stabilized zirconia multilayered films and their optical humidity sensing capabilities based on transmission, *Sensors Actuators B: Chem.* **232** (2016) 283-291.
- [11] R. Wadhene, I.B. Assaker, R. Chtourou, Effect of sulfur quantity in post-treatment on physicals and electrical properties of electrodeposited Kesterite $\text{Cu}_2\text{ZnSnS}_4$ thin films, *J. Mater. Sci. Mater. Electron.* **29** (2018) 17374-17387.
- [12] S.P. Keerthana, R. Yivakkumar, G. Ravi, C.J. Bastina, S. Arun Mehta, D. Velauthapillai, Synthesis of surfactant assisted $\text{Cu}_2\text{ZnSnS}_4$ (CZTS) photocatalysts for removal of dyes from wastewater, *Sustain. Energy Technol. Assessments.* **65** (2024) 1-8.

Publisher's Note: Research Plateau Publishers stays neutral with regard to jurisdictional claims in published maps and institutional affiliations.